

## Influence of Blade Overlap and Blade Angle on the Aerodynamic Coefficients in Vertical Axis Swirling type Savonius Wind Turbine

A. Al-Faruk and A. Sharifian

Computational Engineering and Science Research Centre (CESRC)  
University of Southern Queensland, Toowoomba, Queensland 4350, Australia

### Abstract

When compared with other wind turbines, drag driven vertical axis Savonius wind turbine offers lower power coefficient due to its slow turning speed. However, they have many advantages over others, such as simplicity of manufacturing, ability to operate in any wind direction, and having a good starting torque at low wind speed. They are well suited to be integrated in urban environment as small scale power generating wind mills.

Waste heats or naturally available heat sources such as geothermal and solar energy can be utilized to produce swirling flow when there is a source of angular momentum. Previous computational work suggests that the performance of Savonius turbine can be improved by providing a hot swirling flow inside the turbine chamber. The swirling flow can be induced by a design similar to that of split channels, which includes one or a few vertical slits, and is currently used to onset fire whirls in the laboratories.

In the present experimental study, the influence of blade overlap, blade arc angle and the diameter of the hot air inlet hole on the torque and power coefficient have been investigated. The results indicate that the maximum power coefficient for a 258 mm diameter rotor occurs at 28 mm blade overlap, 195° blade angle and 9 mm diameter of hot air inlet hole.

### Introduction

The demand for wind-power has been increasing exponentially in recent years as a consequence of the quest for low CO<sub>2</sub> emission. Until now, the propeller type horizontal axis wind turbines (HAWTs) have played a primary role in response to this demand. The HAWTs can provide large power outputs, but it needs greater wind velocities and often generate low-frequency noise that can be harmful. In contrast, vertical axis wind turbines (VAWT) are isolated from these environmental problems, resulting in the recent expansion of their use in urban environments. Among a number of VAWTs, the Savonius turbine is known as the most quiet wind power source because it works at the lowest tip-speed ratio [9]. Therefore, they can be employed to generate on-site electricity in city environment. The turbine also easily starts to rotate at low wind speeds because the differential drag on the two blades produces the torque. This allows the turbine to rotate not only at the top of high buildings but also at street level in a city. Since no severe restriction exists for the blade material, the manufacturing process is easy to realize on-site using on-site materials [11,12].

On the other hand, Savonius turbines are widely considered as drag-driven devices. The power extraction efficiency (power coefficient,  $C_p$ ) from the wind is typically in the range of 15 to 20%, which is less than half of the efficiency of HAWTs. This value corresponds to only one third of the Betz's limit of 59.3%. However, it has been observed that at low angles of attack the lift force also contributes to the overall torque generation [6]. Thus, it can be concluded that the Savonius rotor is a combination of a drag-driven and lift-driven device. Therefore, it can go beyond the

limit of power coefficient ( $C_p$ ) of purely drag-driven machines which is 8% [5].

There have been several papers published on the improvement of Savonius turbine performance. Sheldahl et al. [9] reported the data of wind tunnel experiments in which they changed the number of half-cylindrical blades. Kamoji et al. [4] examined the influence of the end plates and the central shaft and found that the power coefficient rose up to 0.21 with the best combination. Saha and Rajkumar [7] confirmed that the twisted blades in the vertical direction provide a better performance than conventional cylindrical blades. To simulate the turbine performance that varies with the Savonius blade configuration, Sargolzaei and Kianifar [8] proposed the application of a neural network algorithm to the modelling of the experimental data. This allows the investigator to predict the power performances without in-depth consideration of fluid dynamics. Another area of improvement is the introduction of wind collection equipment to the space around a turbine [10]. Surrounding a turbine with a guide box succeeded in raising the power coefficient by up to 123% for two blade and 150% for three-blade models relative to the original models [3]. In a similar manner, further significant success was reported using mobile types of solid curtains [2] that recorded 0.38 for the maximum power coefficient. These large improvements are considered to be due to the drag reduction on the returning blade that migrates upstream against the main flow. Recently, Al-Faruk et al. [1] proposed an innovative low cost technique of performance improvement using industrial waste heat. They numerically investigated the possibility of combining fire-whirl mechanism with the primary Savonius wind turbine mechanism by modifying the blade geometry to form a vortex chamber inside the turbine blades. They reported that swirling flows has formed in the chamber when hot air is used instead of fire in a preliminary designed configuration. They compared the performance of the two configurations and reported 25% improvement in power coefficient.

In the present study, experimental investigations have been carried out on the proposed configuration of Al-Faruk et al. [1] to determine the effects geometrical parameters on its performance. Several physical parameters such as blade overlap ratio, blade arc angle, and diameter of hot air inlet of the swirling chamber are considered to determine their effects on the aerodynamics performances in terms of coefficient of power and coefficient of torque. The existing arrangement of experimental set-up allows the performance assessments of the new swirling type Savonius rotor (for ease calling, naming the new configuration as swirling Savonius) as well as conventional Savonius rotor.

### Swirling Savonius Turbine

The swirling Savonius turbine is similar to the classic Savonius turbine which consists of two identical blades of semi-cylinder like surfaces moving them sideways making an overlap in between them as shown in "figure 1". The modification made in swirling Savonius turbine is that unlike the conventional Savonius turbine

which has  $180^\circ$  blade angle, the inner tips of the half cylinders extended further to construct the swirling chamber [1]. The extended angle ( $\theta$ ) of the blades as shown in “figure 1” lowers the air entrainment gap of the vortex chamber. A circular hole of diameter  $d$  made in the bottom end plate act as the hot air inlet of the swirling chamber.

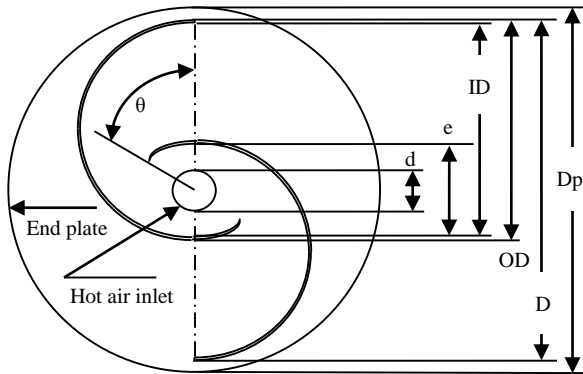


Figure 1. Blade geometry on the bottom end plate of the swirling rotor

Light weight and low cost u-PVC pipe of 150 mm Nominal Diameter has been chosen as the blade material. The mean outside diameter of the pipe was 160 mm and average wall thickness found to be 3 mm. The blades were joined with two circular end plates at the top and bottom ends of the blades. The bottom end plate has been made from 3 mm thick Aluminium sheet, and 3 mm thick Acrylic sheet with a hole at the centre has been used as top end plate to provide a clear top view of the turbine. A circular hole of 44 mm diameter has been cut at the centre of the bottom end plate as the inlet of hot air to the chamber as shown in “figure 1”.

The pipe has been cut into two  $180^\circ$  half cylinder and  $10^\circ$ ,  $15^\circ$ ,  $20^\circ$ ,  $30^\circ$  slots in pairs which were used repeatedly for making different geometrical rotor of swirling Savonius type. After deciding the dimensions of blade geometry such as blade overlap ratio and blade arc angle, the  $180^\circ$  half cylinders were first joined with the end plates by strong adhesive. The inner tip of blades were extended by attaching required arc angled slots with the  $180^\circ$  blades to make the swirling rotor blades. After completing experiments with the same rotor, the components were dismantled and then reassembled for the next experiments. Aluminium sheets were placed on top of the hot air inlet of the swirl chamber to change the diameter ( $d$ ).

The bottom end plate of the turbine was coupled with the end flange of an Aluminium hollow shaft (44 mm inner diameter and 50 mm in length) by six washers and bolts and then the rotor was placed into the ball bearing fixed to the test bench. The use of flanged hollow shaft facilitated easy replacement of rotors. Taking into account the use of one bearing and lack of top shaft, the weight of the rotor was further reduced. Placement of the bearing mechanism closer to the centre of the rotation reduces potential peripheral mass problems and vibrations that could be caused due the miss-balanced assembly.

### Experimental Set-up

The experimental set-up consists of a structural test bench housing the swirling Savonius rotor and the hot air generation chamber, an industrial pedestal fan and measurement devices. A 750 mm diameter industrial pedestal fan used in this work has three speed settings and has the provision to adjust its height. The rotor and some measuring devices have been placed on top of the table and the heating chamber has been placed underneath the table.

The rotor has been supported by one low friction 50 mm bore diameter ball bearing that has been rigidly bolted to the table by

the constructed bearing housing. A stainless steel pipe (50 mm outer diameter and 44 mm inner diameter) has been used as chimney that carries the warm air from the hot air chamber to the bottom of the hollow shaft. Finally the hot air comes out from the chimney to enter the turbine through the hollow shaft. A K-type thermocouple has been inserted through a hole at the top end of the chimney in order to obtain the temperature of the warm air entering into the swirling chamber of the rotor.

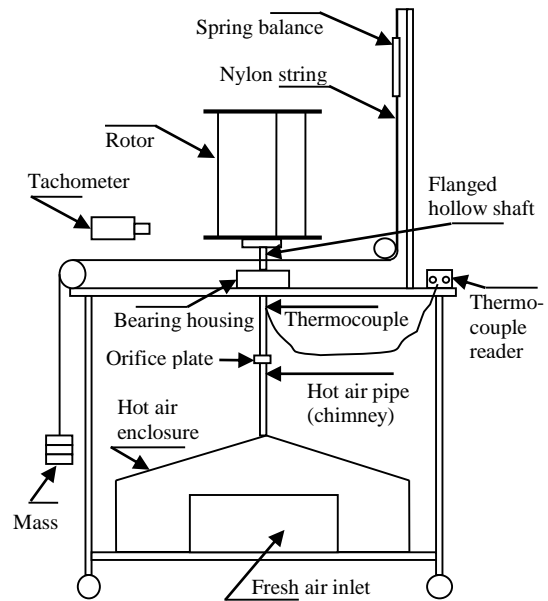


Figure 2. Schematic diagram of experimental set-up

A brake rope dynamometer is used for loading the rotors and subsequently for measuring the rotor’s torque. The brake rope dynamometer is very simple that consists weighing pan, pulleys and spring balance. The spring balance and weighing span is connected by an inelastic string of 0.4 mm diameter running over two pulleys as shown in “figure 2”. The string was wound one turn ( $360^\circ$ ) over the hollow shaft of the rotor on top of the bearing housing.

The heating zone at the bottom of the test table has been fabricated using 0.9 mm stainless steel sheet. Two cooking hot plates were used for heating the air. Only the heating plates were inserted into the enclosure due to safety concerns. To minimize the heat loss to environment from the hot air enclosure and the chimney, room insulation batts has been used to cover outer surfaces. A 250 mm  $\times$  200 mm opening with sliding cover was made in the side wall to allow and control the entry of fresh air into the chamber.

### Experimental Procedure and Data Acquisition

The test bench was placed at 1.8 m downstream of the fan exit such that the centre of the stationary or rotating rotor is in line with the centre of fan exit. It is necessary to produce uniform free stream flow for the rotor as it may affect the stability of swirl generated inside the rotor as well as to reduce the fluctuations of rotor angular velocity. Wind velocities at 35 cm upstream and 35 cm downstream from the central axis were measured at nine points located systematically in the projection area of the rotor blade. Then the average value of each projected area were averaged to obtain the wind velocity used to calculate the performance parameters.

The rotors were allowed to rotate from no load condition and the maximum rotational speed is recorded by a tachometer when the rotor reached steady state condition. The rotors was loaded gradually (adding 50 gm of mass each time) by the rope brake dynamometer from no load condition to the highest load that

stopped the rotor. The spring balance readings of the dynamometer, dead weights and maximum steady state rotational speeds of the rotor were recorded and used to calculate the transmitted load/torque, brake power. Finally the performance parameters as a function of the tip speed ratio were analysed.

The dimensionless performance parameters commonly used in the aerodynamics of wind turbines are coefficient of power ( $C_p$ ) and coefficient of torque ( $C_t$ ) which are usually determined as a function of dimensionless tip speed ratio ( $\gamma$ ). The definitions are as follows:

$$C_p = \frac{P}{\frac{1}{2}\rho DHU^3}, C_t = \frac{T}{\frac{1}{4}\rho D^2 HU^2} \text{ and } \gamma = \frac{\omega D}{2U}$$

where  $\rho$  is the air density,  $U$  wind velocity,  $P$  mechanical power,  $H$  rotor height, and  $D$  rotor diameter.

## Results and discussions

Experimental tests have been carried out over 50 rotors with different geometries. The results have been analysed based on the influence of the parameters on the power and torque coefficients and then compared the performance with the conventional Savonius rotor.

### Effect of Blade Overlap Ratio

The blade overlap ratio ( $\beta$ ), which is defined by the ratio of blade overlap distance ( $e$ ) and the inner diameter ( $ID$ ) of the blade (refer to “figure 1”), has the most significant influence on the performance of swirling Savonius turbine. The blade overlap ratios studied in this experiments are 0.15, 0.20, 0.25, 0.31, and 0.41.

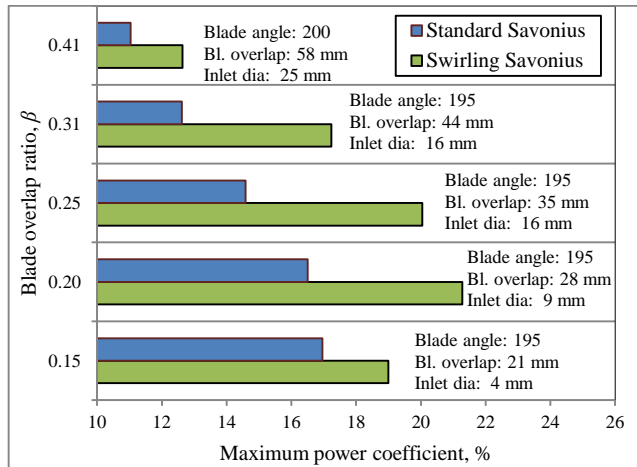


Figure 3. Comparison of maximum power coefficient between conventional and swirling Savonius turbine at different blade overlap ratio

The maximum power coefficient found at different blade overlap ratios has been plotted for both standard and swirling Savonius turbines and the optimum parameters noted in “figure 3”. The maximum power coefficient found for conventional Savonius rotor was 16.96% at 0.15 blade overlap ratio and drops its value with the increase of blade overlap ratio. The decrease of maximum power coefficient with blade overlap ratio for conventional Savonius rotor is aligned with the previous reports found in the literature. On the other hand, for swirling Savonius rotor maximum power coefficient at 0.15 blade overlap ratio is lower than that of 0.20 but then decreases with the increase of blade over ratio. The maximum power coefficient of swirling Savonius rotor found in this study is 21.28% occurred at 0.20 blade overlap ratio with 9 mm diameter inlet and 195° blade arc angle. “Figure 3” suggest that for all blade overlap, the power coefficient of swirling Savonius rotor is larger than the corresponding values of conventional Savonius rotor.

As the diameter of the rotor can be calculated using the formula of  $D = OD + ID(1 - \beta)$ , for same blade inside and outside diameters, rotor diameter depends on blade overlap ratio. With the increase of blade overlap ratio, the positive moment generating concave blade’s swept area reduces but negative convex blade’s swept area remain constant which results lower overall moment on the shaft of rotor. For this reason  $C_p$  reduces with the increase of overlap ratio for conventional turbine. However, for swirling Savonius turbine, as the vortex generated in the blade overlapping zone which compensate the loss as well as promotes the performance up to certain optimum point of overlap ratio.

### Effect of Hot Air Inlet Diameter

The diameter of the circular hole at the bottom end plate which is the hot air inlet for of the swirling chamber was initially 44 mm. The other diameters tested in the experiments were 4, 9, 16, 25, 31, and 38 mm. The maximum power coefficients at different hot air inlet diameter for three different blade arc angles have been plotted for the optimum configuration of 0.20 blades overlap ratio (28 mm blade overlap) in “figure 4”. The power coefficient reached maximum value for smaller diameter of hot air inlet, in this case 9 mm for all three blade arc angles. The reason is that when the hot air inlet diameter reduced for the same approximate amount of mass flow rate, the inlet velocity increases that generates strong swirling flow in the chamber, and subsequently increases the power coefficient. However, higher inlet diameter of hot air is required when the blade overlap distance increases for maximum power coefficient as presented in “figure 4”.

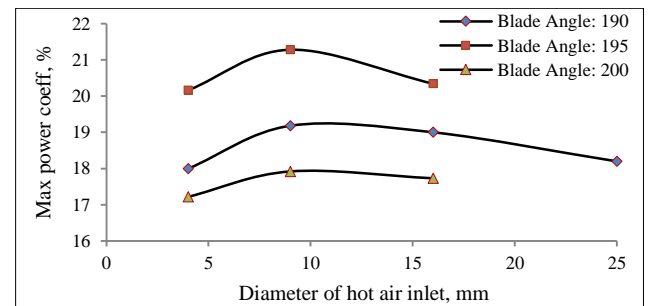


Figure 4. Distribution of maximum power coefficient with hot air inlet diameter for different blade arc angles at 28 mm blade overlap rotor

### Effect of Blade Arc Angle

Experiments were carried out on the conventional Savonius rotor of 180° blade arc angle as well as swirling Savonius rotors in order to make performance comparisons between them. The blade arc angles of swirling Savonius rotors in this study are 180°, 190°, 195°, 200°, and 210°. So the blade’s inner tip extensions ( $\theta$ ) are 0°, 10°, 15°, 20°, and 30° respectively.

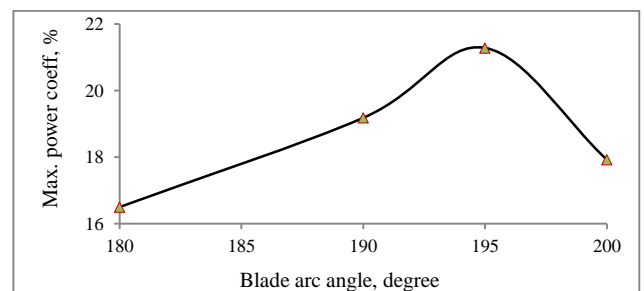


Figure 5. Variation of maximum power coefficient with rotor blade angle at 28 mm blade overlap and 9 mm diameter of hot air inlet

“Figure 5” presents the maximum power coefficients for the rotor configuration of 0.20 blade overlap ratio and with 9 mm diameter hot air inlet for three different blade arc angles ranging from 190° to 200° as well as conventional 180° rotor. With the increase of

blade arc angle, power coefficient increases but after reaching a maximum values, it declines. The increase of blade arc angle increases the mass and the mass moment of inertia of the rotor might be the reason for lower performance. It also reduces the entrance passage of free stream wind into circulation zone.

### Comparison of Swirling and Conventional Savonius

The best features of conventional and swirling Savonius turbines are compared in terms of steady state angular velocities, and power and torque coefficients.

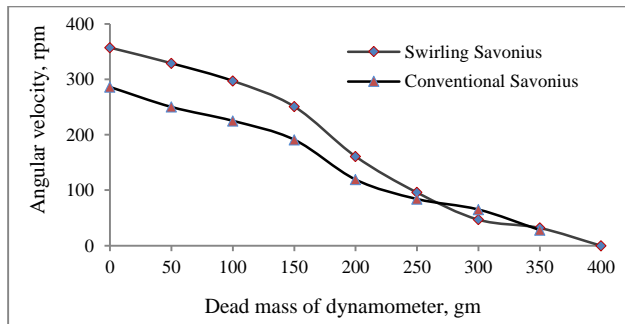


Figure 6. Steady state angular velocity of rotors at different suspended dead mass of rope brake dynamometer

The maximum steady state angular velocities versus suspended dead mass of dynamometer are plotted in “figure 6”. The figure demonstrates that no load maximum speed of swirling rotor is higher (357 rpm) than the conventional rotor (286 rpm). With the increase of suspended mass, the differences in speed values drops and the values are almost the same before stopping. This performance suggests that, swirling flow may not be generated at lower angular velocities but grew stronger with the increase of angular velocity.

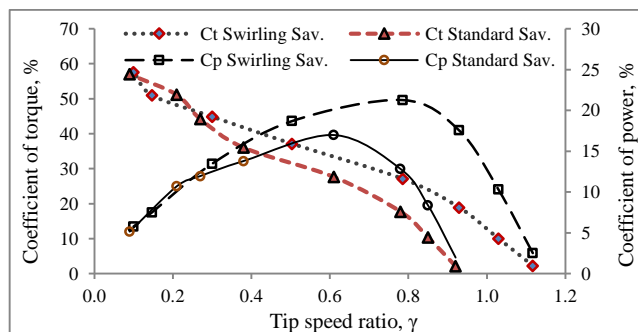


Figure 7. Variation of torque and power coefficients with tip speed ratio of a rotor of 28 mm blade overlap, 9 mm diameter hot air inlet and 195° blade arc angle and the conventional Savonius rotor

“Figure 7” represents the coefficients of torque and power plotted against the tip speed ratios for the optimum swirling and standard Savonius configurations. The maximum torque coefficients for both turbines are nearly the same value of over 57%, but the differences extends with higher tip speed ratio. The tip speed ratio at no dead load of swirling Savonius turbine is 1.12 which is 22% higher than the conventional Savonius turbine.

The plot of power coefficient versus rotor tip speed ratio for optimum swirling and conventional Savonius rotors demonstrates that for lower tip speed ratios the values are the same, but difference is widening with the increase of steady state speeds of rotor. The maximum power coefficient (21.28%) found at 0.78 tip speed ratio for swirling turbine whereas for Savonius turbine,

maximum power coefficient (16.96%) occurred at 0.61. From those plots it can be deduced that at lower speeds of swirling turbine, the swirling flow might not be generated due to the strong free stream wind which may swept away the hot air before the generation of circulation.

### Conclusions

The effects of several geometrical parameters on the aerodynamic performances have been investigated and maximum power coefficient obtained at 0.20 blade overlap ratio (28 mm blade overlap), 9 mm hot air inlet diameter with 195° arc angle of blades. The results comparison between the optimum swirling and conventional Savonius turbine suggest that power coefficient of swirling turbine is increased by 25.5% than the conventional turbine. However, at lower angular velocities performances of swirling and Savonius turbine remains the same.

### References

- [1] Al-Faruk, A., Sharifian, A. & Atresh, S., Numerical investigation of performance of a new type of Savonius turbine, *18th Australasian Fluid Mechanics Conference*, Launceston, 2012.
- [2] Altan, B.D., Atilgan, M. & Ozdamar, A., An experimental study on improvement of a Savonius rotor performance with curtaining, *Experimental Thermal and Fluid Science*, 32, 2008, 1673-1678.
- [3] Irabu, K. & Roy, J.N., Characteristics of wind power on Savonius rotor using a guide-box tunnel, *Experimental Thermal and Fluid Science*, 32, 2007, 580-586.
- [4] Kamoji, M.A., Kedare, S.B. & Prabhu, S.V., Experimental investigations on single stage modified Savonius rotor. *Applied Energy*, 86, 2009, 1064-1073.
- [5] Manwell, J., McGowan, J. & Rogers, A., Wind energy explained: theory, design and application, Wiley, 2010.
- [6] Modi, V. & Fernando M., On the performance of the Savonius wind turbine, *Journal of Solar Energy Engineering*, 111(1), 1989, 71-81.
- [7] Saha, U.K. & Rajkumar, M.J. On the performance analysis of Savonius rotor with twisted blades, *Renewable Energy*, 31, 2006, 1776-1788.
- [8] Sargolzaei, J. & Kianifar, A., Modeling and simulation of wind turbine Savonius rotors using artificial neural networks for estimation of the power ratio and torque, *Simulation Modelling Practice and Theory*, 17, 2009, 1290-1298.
- [9] Sheldahl, R.E., Blackwell, B.F. & Feltz, L.V. Wind tunnel performance data for two and three-bucket Savonius rotors. *Journal of Energy*, 2, 1978, 160-164.
- [10] Ushiyama, I., Nagai, H. & Shionoda, J., Experimentally determining the optimum design configuration for Savonius rotors, *transaction of the Japan society of mechanical engineers. Series B*, 52-480, 1986, 2973-2981 [in Japanese].
- [11] Valdes, L.C. & Darque, J., Design of wind-driven generator made up of dynamos assembling, *Renewable Energy*, 28, 2003, 345-62.
- [12] Valdes, L.C. & Raniriharinosy, K. Low technical wind pumping of high efficiency, *Renewable Energy*, 24, 2001, 275-301.